Pflugers Arch - Eur J Physiol (2011) 462:559–571
DOI 10.1007/s00424-011-0998-2

Functional arrangement of the 12th transmembrane region in the CFTR chloride channel pore based on functional investigation of a cysteine-less CFTR variant

Feng Qian · Yassine El Hiani · Paul Linsdell

Received: 26 May 2011 / Revised: 27 June 2011 / Accepted: 15 July 2011 / Published online: 28 July 2011

Abstract The membrane-spanning part of the cystic fibrosis transmembrane conductance regulator (CFTR) Cl^- channel comprises 12 transmembrane (TM) α-helices, arranged into two pseudo-symmetrical groups of six. While TM6 in the N-terminal TMs is known to line the pore and to make an important contribution to channel properties, much less is known about its C-terminal counterpart, TM12. We have used patch clamp recording to investigate the accessibility of cytoplasmically applied cysteine-reactive reagents to cysteines introduced along the length of TM12 in a cysteine-less variant of CFTR. We find that methanethiosulfonate (MTS) reagents irreversibly modify cysteines substituted for TM12 residues N1138, M1140, S1141, T1142, Q1144, W1145, V1147, N1148, and S1149 when applied to the cytoplasmic side of open channels. Cysteines sensitive to internal MTS reagents were not modified by extracellular [2-(trimethylammonium)ethyl] MTS, consistent with MTS reagent impermeability. Both S1141C and T1142C could be modified by intracellular [2-sulfonatoethyl] MTS prior to channel activation; however, N1138C and M1140C, located deeper into the pore from its cytoplasmic end, were modified only after channel activation. Comparison of these results with previous work on CFTR-TM6 allows us to develop a model of the relative positions, functional contributions, and alignment of these two important TMs lining the CFTR pore. We also propose a mechanism by which these seemingly structurally symmetrical TMs make asymmetric contributions to the functional properties of the channel pore.

F. Qian and Y. El Hiani contributed equally to this work.

F. Qian · Y. El Hiani · P. Linsdell (✉)
Department of Physiology & Biophysics, Dalhousie University,
1459 Oxford Street,
Halifax, Nova Scotia B3H 4R2, Canada
e-mail: paul.linsdell@dal.ca

Keywords Chloride channel · Cystic fibrosis transmembrane conductance regulator · Ion channel pore · Permeation · Site-directed mutagenesis · Substituted cysteine accessibility · Patch clamp

Introduction

Cystic fibrosis is the result of genetic mutations that cause dysfunction of the cystic fibrosis transmembrane conductance regulator (CFTR) protein. CFTR, a member of the ATP-binding cassette (ABC) family of membrane transport proteins, functions as an epithelial cell Cl^- channel necessary for transepithelial salt and water transport in many organs [12]. As with other ABC proteins, CFTR exhibits a modular architecture of two transmembrane domains (TMDs) made up of six α-helical membrane-spanning regions each and two cytoplasmic nucleotide binding domain (NBDs). The two TMDs of ABC proteins come together to form a single transmembrane pathway for the movement of substrate [36], namely, Cl^- and other small anions in the case of CFTR [22].

The overall architecture of the CFTR Cl^- channel pore region and the contributions of different individual transmembrane α-helices (TMs) to the pore are not known. Current structural models of CFTR suggest that the two TMDs are arranged in a symmetrical manner [34, 37], consistent with the known structures of other ABC proteins [18, 28, 36]. However, the two TMDs have been described as functionally asymmetric, with the N-terminal TMD (TMD-1, comprising TMs 1–6) being thought to be more important in determining the functional properties of the channel pore than the C-terminal TMD (TMD-2, comprising TMs 7–12) [22]. Much work has focused on TMs 1 and 6, both in TMD-1, both of which clearly make important contributions to the pore [13, 22]. Whereas TM6

is generally thought of as being of prime importance in the CFTR pore [3–5, 9, 22, 29], much less attention has been paid to its counterpart in TMD-2, namely, TM12, and evidence that this TM influences pore properties is much more limited [11, 15, 16, 30, 31, 40, 43, 45]. In fact, a direct comparison of the functional roles played by TMs 6 and 12 concluded that TMD-1 is much more important in determining the permeation phenotype of the channel than TMD-2 [15]. Furthermore, while the substituted cysteine accessibility mutagenesis (SCAM) approach has been used extensively to identify pore-lining amino acid side chains in TMD-1 [1–5, 7, 9, 41], this same approach has been used only in a very limited fashion in TMD-2 [11, 45].

Recent work from our laboratory has begun to build a three-dimensional functional model of the CFTR pore region, based on work on a cysteine-less CFTR variant [41, 45]. However, in order to develop such models, much more information on the location and orientation of other TMs around the pore—especially those from TMD-2—is required. Previously, we used a SCAM-based approach to identify pore-lining amino acids in TM6 and to characterize the orientation and of this TM around the CFTR pore [9]. Given the supposed structural symmetry between the two TMDs, we now present a similar analysis of TM12. Our results indicate that TM12 makes an extensive contribution to the inner vestibule of the CFTR pore, including to a "barrier" within the pore that prevents access of cytoplasmic substances in non-activated channels. However, the contribution of TM12 to the putative narrow region of the pore appears conspicuously less than that of TM6. Our results also allow us to model the orientation and position of TM12 in TMD-2 in the overall architecture of the CFTR pore.

Materials and methods

Experiments were carried out on baby hamster kidney (BHK) cells transiently transfected with CFTR. As in our recent study on CFTR-TM6 [9], we have used a human CFTR variant ("cys-less" CFTR) in which all endogenous cysteine residues had been substituted by other amino acids [32] and which also includes a mutation in NBD1 (V510A) to increase protein expression in the cell membrane [19]. Use of cys-less CFTR is necessary for these studies because wild-type CFTR is potently inhibited by cytoplasmic methanethiosulfonate (MTS) reagents [39]. While the functional properties of cys-less and wild-type CFTR have been described as very similar [3, 8, 32], differences have been reported, with cys-less CFTR showing a significantly greater single channel conductance than wild type [8, 19, 32]. Mutagenesis was carried out using the QuikChange site-directed mutagenesis system (Stratagene, La Jolla, CA, USA) and verified by DNA sequencing. Transfection and cell culture were carried out as described recently [19].

Macroscopic CFTR currents were recorded using patch-clamp recording from inside–out membrane patches excised from BHK cells as described in detail previously [23, 24]. Following patch excision, any pretreatment of the inside–out patch if necessary (see below), and recording of background currents, CFTR channels were activated by exposure to protein kinase A (PKA) catalytic subunit (20 nM) plus MgATP (1 mM) in the cytoplasmic solution. CFTR channel activity was then further increased by the addition of 2 mM sodium pyrophosphate (PPi). Pyrophosphate was used to maximize and stabilize macroscopic current amplitude, which was very small for many TM12 mutants, and so increase resolution. Both intracellular (bath) and extracellular (pipette) solutions contained 150 mM NaCl, 2 mM $MgCl_2$, and 10 mM *N*-tris (hydroxymethyl)methyl-2-aminoethanesulfonate (TES) (pH adjusted to 7.4 using NaOH). Channels were exposed to intracellular and extracellular cysteine-reactive MTS reagents to covalently modify introduced cysteine side chains. Two MTS reagents, the negatively charged [2-sulfonatoethyl] MTS (MTSES) and the positively charged [2-(trimethylammonium)ethyl] MTS (MTSET), were used. These reagents were initially prepared as high concentration (160 mM) stock solutions in distilled water and stored frozen as small volume aliquots until the time of use, when they were diluted in bath solution and used immediately.

Initially, high concentrations of MTS reagents (200 μM MTSES or 2 mM MTSET) that we have previously found to be without effect on cys-less CFTR currents [9, 19, 41, 45] were applied to the cytoplasmic face of inside–out membrane patches following maximal channel activation, and currents were monitored for at least 5 min until the current had again reached a steady amplitude (see Fig. 1a). To measure the rate of modification of open channels (see Fig. 3), macroscopic current amplitude was monitored continuously, and the time-dependent change in amplitude following addition of MTSES was fitted by a single exponential function. In cases where the rate of modification was very fast, the concentration of MTSES used was reduced to 20 μM. The time constant of exponential current decay, τ, was used to calculate the apparent second order reaction rate constant, k, from the equation $k=1/([\mathrm{MTSES}]\tau)$.

In some cases, MTS reagents were used to pretreat intact cells (external application; Fig. 4) or inside–out membrane patches (internal application; Fig. 5) before recordings. In Fig. 4, channels were pretreated with external MTSET. Intact cells were preincubated in 5 mM MTSET (in normal bath solution) for 5 min, following which cells were washed thoroughly with bath solution and transferred to the recording chamber for patch clamp

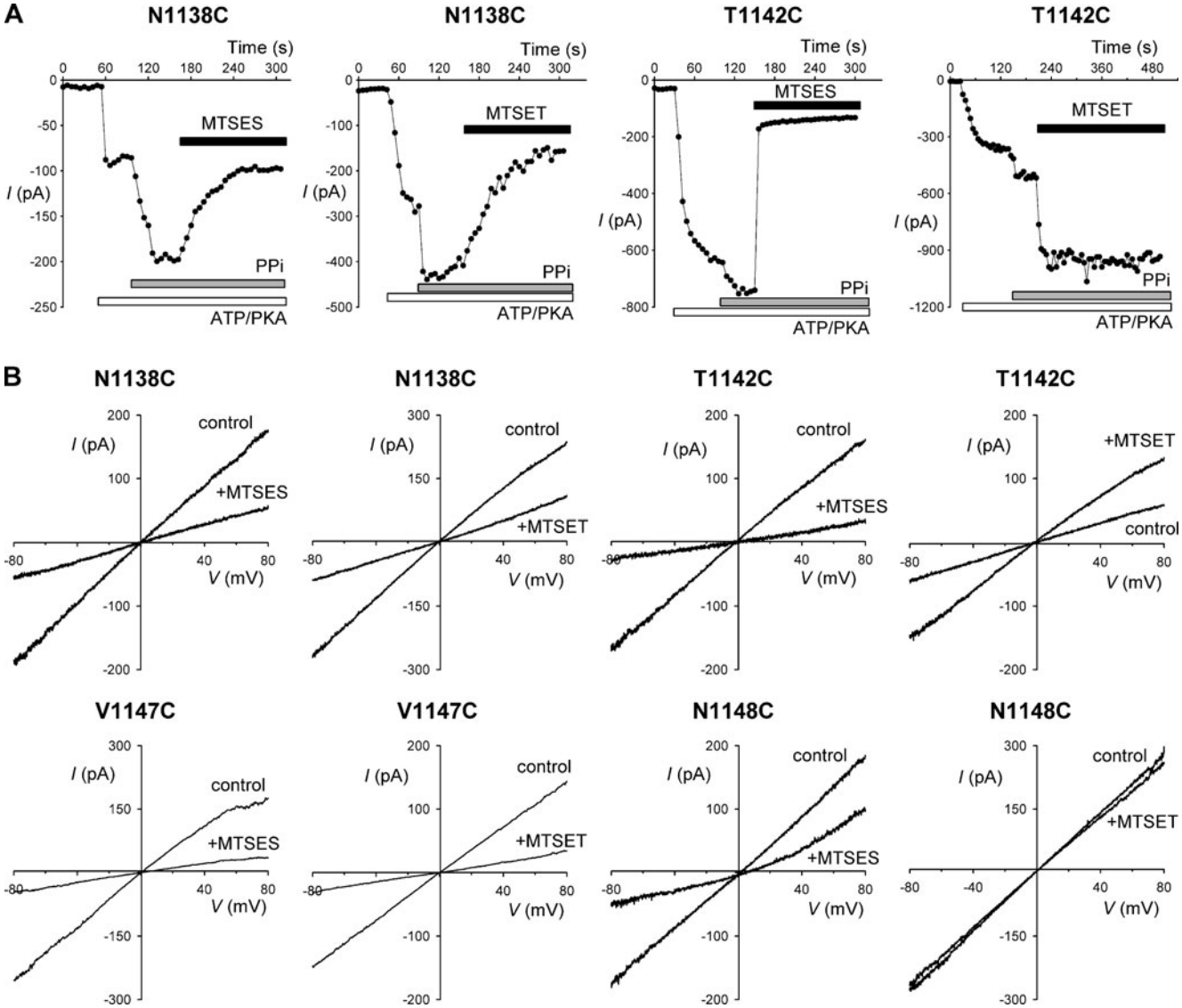

Fig. 1 Modification of cysteine-substituted CFTR-TM12 mutants by internal MTS reagents. **a** Example time courses of macroscopic currents (measured at −80 mV) carried by N1138C and T1142C as indicated in inside–out membrane patches. Following patch excision and recording of baseline currents, patches were treated sequentially with PKA and ATP (as indicated by the *white bar* at the bottom of each panel), PPi (*gray bar*), and either MTSES (200 μM) or MTSET (2 mM) (*black bar*), leading to rapid inhibition (N1138C+MTSES, N1138C+MTSET, and T1142C+MTSES) or augmentation (T1142C+MTSET) of macroscopic current amplitude. Lack of effect of these concentrations of MTSES and MTSET in cys-less CFTR under identical conditions was shown in our recent publications [9, 41]. **b** Example leak subtracted *I–V* relationships for N1138C, T1142C, V1147C, and N1148C, recorded from inside out membrane patches following maximal channel activation with PKA, ATP, and PPi. In each panel, currents recorded before application of MTS reagents (control) and after full modification by intracellular MTSES (200 μM) or MTSET (2 mM) had been achieved. As described in the text, whereas MTSES application always led to a decrease in macroscopic current amplitude in reactive mutants, the effects of MTSET were to decrease (e.g., N1138C, V1147C), increase (e.g., T1142C) or not significantly alter (e.g., N1148C) macroscopic current amplitude. Again, lack of effect of these concentrations of MTSES and MTSET on cys-less CFTR under identical experimental conditions has been shown recently [9, 41, 45]

analysis. MTSET was used in these experiments as we have previously found it to be a less state-dependent probe of the outer pore than MTSES [10]. Indeed, we have previously used a similar MTSET pretreatment protocol to identify positively a number of externally accessible sites in CFTR [9, 10, 44].

In Fig. 5, channels were pretreated with internal MTSES, using one of two pretreatment protocols described previously [9, 41]. Following patch excision to the inside–out configuration, 200 μM MTSES was added to the cytoplasmic (bath) solution. MTSES was applied alone (for modification of non-activated channels) (Fig. 5c) or

together with PKA (20 nM) and ATP (1 mM) (for modification of activated channels) (Fig. 5b). After a 2-min treatment period, all substances were washed from the bath using normal bath solution. Following recording of background leak currents, CFTR channels were then activated using PKA (20 nM), ATP (1 mM), and PPi (2 mM) as usual, and then exposed to a test treatment of MTSES. Although this approach does not quantify the rate of modification of non-activated channels, it does provide a simple separation of side chains that are readily modified in non-activated channels versus those for which the rate of modification in non-activated channels is negligible (see [9, 41]). Pretreatment for 2 min with 200 μM MTSES is expected to result in ~100% modification in fully activated channels (see Fig. 3).

Current traces were filtered at 100 Hz using an 8-pole Bessel filter, digitized at 250 Hz, and analyzed using pCLAMP-10 software (Molecular Devices, Sunnyvale, CA, USA). Macroscopic current–voltage (*I–V*) relationships were constructed using depolarizing ramp protocols [25] from a holding potential of 0 mV. Background (leak) currents recorded before addition of PKA and ATP have been subtracted digitally, leaving uncontaminated CFTR currents [14, 25].

Experiments were carried out at room temperature (21–24° C). Values are presented as mean±SEM. Tests of significance were carried out using a Student's two-tailed *t* test unless stated otherwise. All chemicals were from Sigma-Aldrich (Oakville, ON, Canada), except for PKA (Promega, Madison, WI, USA) and MTSES and MTSET (Toronto Research Chemicals, North York, ON, Canada).

Results

Accessibility of cysteines introduced into TM12

Recently, we have used internal application of MTS reagents to identify pore-lining cysteine side chains introduced into TM1 [41] and TM6 [9] in TMD-1 of cys-less CFTR. In the present study, we used a similar approach to identify pore-lining side chains in TM12 in TMD-2. We used site-directed mutagenesis to substitute cysteines for each of 19 consecutive amino acids in TM12, from I1131 near the putative extracellular end to S1149 near the intracellular end of this TM. Expression of each of these 19 cysteine-substituted mutants in BHK cells led to the appearance of macroscopic ATP- and PKA-dependent, PPi-stimulated currents in inside–out membrane patches (eg. Fig. 1a).

Application of MTSES (200 μM) or MTSET (2 mM) to the intracellular solution after channel activation with PKA, ATP, and PPi significantly altered macroscopic current amplitude in nine out of 19 cysteine-substituted mutants tested (N1138C, M1140C, S1141C, T1142C, Q1144C, W1145C, V1147C, N1148C, and S1149C; Figs. 1 and 2). The pattern of functional effects of modification in TM12 fell into three different groups depending on the location of the mutation in the primary amino acid sequence (Figs. 1 and 2). In the central region of TM12 (N1138C, M1140C, and S1141C), macroscopic current amplitude was decreased by both MTSES and MTSET (Figs. 1 and 2). A similar functional effect was observed for cysteines introduced into the analogous region of TM6 [9] and was proposed to represent occlusion of a relatively restricted region of the pore following modification by the bulky MTS reagents. Closer to the intracellular end of TM12 (in T1142C, Q1144C, and W1145C), macroscopic current amplitude was decreased by MTSES application but increased by MTSET (Figs. 1 and 2). Again, a similar pattern was previously observed close to the cytoplasmic end of TM6 [9]. However, unlike previous findings in TM6 [9], we observed a third pattern for cysteines introduced closest to the putative cytoplasmic end of TM12 (V1147C, N1148C, and S1149C). Here, macroscopic current amplitude was decreased by MTSES application but either decreased (V1147C, S1149C) or not significantly affected (N1148C) by MTSET application. In each case, the effects of MTS reagents were not reversed by washing these reagents from the bath (see also Fig. 5); however, as described previously in TM6 [9], the effects of MTS reagents could be reversed by the addition of 2–5 mM dithiothreitol (DTT). These concentrations of MTSES and MTSET had no effect on macroscopic current amplitude in cys-less CFTR (Fig. 2), as shown previously using similar protocols [9, 41], although it has been shown that higher concentrations of MTSES (>1 mM) cause a reversible, voltage-dependent block of cys-less CFTR [19]. A similar lack of effect following prolonged (>5 min) exposure to such high concentrations of both MTSES and MTSET was also observed in ten out of 19 cysteine-substituted mutants tested (I1131C, I1132C, L1133C, T1134C, L1135C, A1136C, M1137C, I1139C, L1143C, and A1146C). The effects of MTS reagents on the amplitude of macroscopic currents carried by different channel constructs are summarized in Fig. 2.

For MTS reagent-sensitive TM12 mutants located relatively deeply into the pore from its cytoplasmic end (N1138C, M1140C, S1141C, and T1142C), the rate of modification was estimated from the time course of macroscopic current amplitude change following application of MTSES (20–200 μM). As shown in Fig. 3a, modification was rapid in M1140C, S1141C, and T1142C, even using a low concentration of MTSES (20 μM), and noticeably slower in N1138C, even with 200 μM MTSES. The overall pattern of calculated modification rate constants

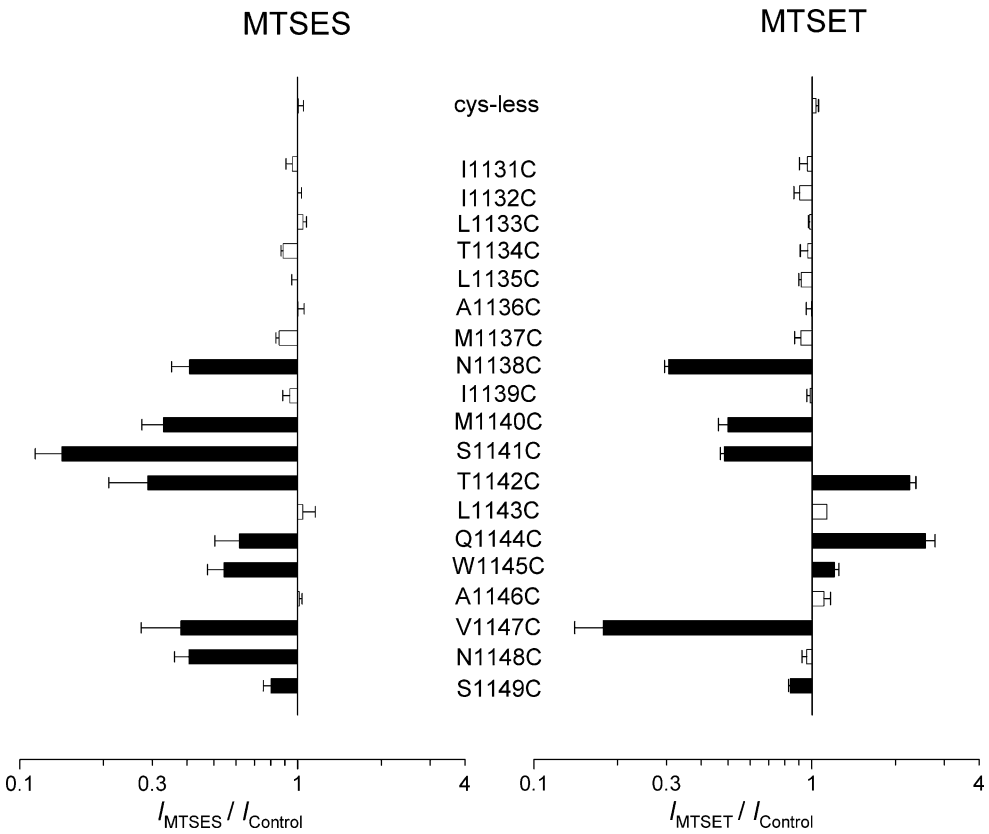

Fig. 2 Effects of internal MTS reagents on cysteine-substituted CFTR-TM12 mutants. Mean effect of treatment with 200 μM MTSES (*left*) or 2 mM MTSET (*right*) on macroscopic current amplitude in cys-less CFTR and in each of 19 different cysteine substituted TM1 mutants. Effects of these two MTS reagents were quantified by measuring current amplitudes at membrane potentials of +80 mV (for MTSES, *left*) and −80 mV (for MTSET, *right*) before MTS reagent application and after complete modification had taken place. *Black bars* represent a significant difference from cys-less ($p<0.05$), *white bars* no significant difference. Mean of data from three to five patches

shown in Fig. 3b suggests that modification is faster for cysteines introduced closer to the cytoplasmic end of TM12 and slower at N1138C located further along the axis of TM12.

Side and state dependence of modification

MTS reagents are not permeant in CFTR [3, 5, 9]; however, we identified three sites in the central part of TM6 at which introduced cysteines could be modified by both internally and externally applied MTS reagents [9]. To gain some information on the orientation of TM12 in the CFTR pore, we therefore examined whether the outermost cysteines introduced into this TM that were sensitive to internal MTS reagents (N1138C, M1140C, and S1141C) could also be modified by extracellular MTSET. Using the same approach that we used previously in TM1 [41] and TM6 [9], we sought to identify sites at which pretreatment with extracellular MTSET would prevent subsequent modification by intracellular MTSET. As described previously [9, 41], intact cells were exposed to a high concentration of MTSET (5 mM) for 5 min. Cells were then washed and transferred to the experimental chamber for patch clamp analysis. After patch excision to the inside–out configuration, CFTR channels were activated using PKA, ATP, and PPi and subsequently treated with intracellular MTSET (2 mM), exactly as in Fig. 1. As shown in Fig. 4a, patches excised from MTSET-pretreated cells expressing N1138C, M1140C, or S1141C all gave macroscopic currents that were decreased in amplitude following addition of 2 mM MTSET to the intracellular solution. In fact, as shown quantitatively in Fig. 4b, these currents showed indistinguishable sensitivity to intracellular MTSET to those recorded from patches excised from cells that had not been pretreated with extracellular MTSET. These results suggest that none of N1138C, M1140C, or S1141C can be modified covalently by extracellular MTSET.

Our previous work using intracellular MTSES to modify cysteines introduced into other TMs also identified some sites at which modification occurred only following channel activation, suggesting that a state-dependent conformational change controls access of internally applied MTS reagents into the pore [9, 41]. State dependence of modification was most readily apparent using a pretreatment protocol, in which cysteines introduced at some sites were modified during pretreatment of inside–out patches with intracellular MTSES, whereas others were apparently not modified unless the pretreatment also included PKA and ATP to promote channel activation [9, 41]. We used a similar approach to determine whether N1138C, M1140C, S1141C, and T1142C, located relatively deeply into the pore from its cytoplasmic end and all strongly sensitive to inhibition by intracellular MTSES (Figs. 2 and 3), could be modified by MTSES pretreatment. Figure 5a shows examples of the

strong inhibition of each of these mutants by 200 μM MTSES in patches that had received no pretreatment. In each case, inhibition was very fast after addition of MTSES, and modification appeared complete in <2 min (see also Fig. 3). Figure 5b and c shows the effects of MTSES application under similar conditions after channel activation with PKA, ATP, and PPi, but in inside–out patches that had been pretreated with intracellular MTSES (200 μM, for a 2 min pretreatment period) under two different sets of conditions (see Materials and methods). In Fig. 5b, patches were pretreated with MTSES in the presence of PKA and ATP after patch excision, whereas in Fig. 5c inside–out patches were pretreated with MTSES alone. In this way, we expect MTSES applied during the pretreatment period to have access to activated channels in Fig. 5b, but only to non-activated channels in Fig. 5c [9, 41]. In both cases, following the 2-min pretreatment period, all drugs were thoroughly washed from the bath, and channels were activated by PKA, ATP, and PPi before application of a second, test exposure to MTSES. In patches that had been pretreated with MTSES, PKA, and ATP and then washed, currents carried by each of these four mutants were insensitive to the second, test exposure to MTSES (Fig. 5b), suggesting that channels had been covalently modified by MTSES during the pretreatment period and that this modification had not been reversed by washing the MTSES from the bath. However, different results were obtained when patches were pretreated with MTSES in the absence of PKA and ATP (Fig. 5c). Both S1141C and T1142C channels were again rendered insensitive to the test exposure to MTSES, again consistent with them having been covalently modified during pretreatment. In contrast, currents carried by both N1138C and M1140C were strongly inhibited by application of the test dose of MTSES, suggesting that they had not been covalently modified by MTSES pretreatment. These results, which are summarized quantitatively in Fig. 5d, suggest that while S1141C and T1142C can be modified by MTSES prior to channel activation, N1138C and M1140C are modified by MTSES only very slowly, if at all, in channels that have not been activated by PKA and ATP.

Discussion

While it has long been suggested that TM12 should line the CFTR pore [17, 29], this suggestion has not previously been tested in a systematic fashion. Our present results indicate that TM12 lines a large part of the cytoplasmically accessible region of the cys-less CFTR pore in the open state (summarized in Fig. 6). Within this region, cysteines substituted for nine out of 12 consecutive amino acid side chains (N1138, M1140, S1141, T1142, Q1144, W1145, V1147, N1148, and S1149) can be modified by intracellular MTS reagents, leading to a change in channel function. Cytoplasmically applied MTS reagents do not appear to modify cysteines introduced closer to the outside of TM12 (i.e., at I1131–M1137), suggesting that MTS reagents cannot penetrate beyond N1138 in open channels. Extracellular MTSET did not appear able to modify the outermost of these internal MTS-sensitive cysteines (N1138C, M1140C, and S1141C; Fig. 4), consistent with MTS reagents not being permeant. Previous work from our group suggested that externally applied MTS reagents could modify cysteines only in the outermost part of TM12, namely, I1131C and I1132C [11]; these same cysteines were insensitive to internally applied MTS reagents (Fig. 2), again consistent with impermeability to these reagents. These results therefore suggest a functional division of TM12 in cys-less CFTR (Fig. 6) into an externally accessible part (I1131–I1132), an internally accessible part (N1138–S1149), and an "inaccessible" part (L1133–M1137) that apparently forms a barrier to the movement of MTS reagents through the pore. Given that MTS reagents are not permeant, it has previously been suggested that such a barrier represents a constricted region of the pore that is too narrow to allow passage of bulky MTS reagents [3, 9, 41]. It therefore seems reasonable to assume that the narrowest part of the open channel pore is located somewhere between L1133 and M1137.

Cytoplasmically applied MTS reagents were able to modify cysteines introduced at most sites in the inner part of TM12, with modification being observed at nine out of 12 consecutive residues in the region N1138–S1149 (Fig. 2). The large proportion of apparently pore-lining side chains seems inconsistent with the proposed α-helical structure of this TM. It is possible that this region does not adopt an α-helical conformation or that a very wide arc of the α-helix comes into contact with the aqueous lumen of the inner vestibule of the pore. However, we feel that a more likely explanation is that TM12 forms an α-helix that exhibits considerable rotational movement, allowing for different faces of the α-helix to be exposed to the pore at different times. A rotational movement of this kind has previously been suggested to occur in TM6 [4].

Figure 6 also compares the pattern accessibility of cysteines introduced into TM12 with our previous findings in TM6 (Fig. 6a) and TM1 (Fig. 6b) of cys-less CFTR. The proposed alignment of these TMs is based on a number of factors, including access to internally and externally applied MTS reagents, rate of modification by internal MTSES, apparent state dependence of modification by internal MTSES, and previous cross-linking studies. Residues accessible to MTS reagents only from the extracellular side of the membrane (colored green in Fig. 6) appear to be restricted to the outermost end of these TMs—R104 in TM1, R334, K335, and I336 in TM6, and I1131 and I1132 in TM12. In

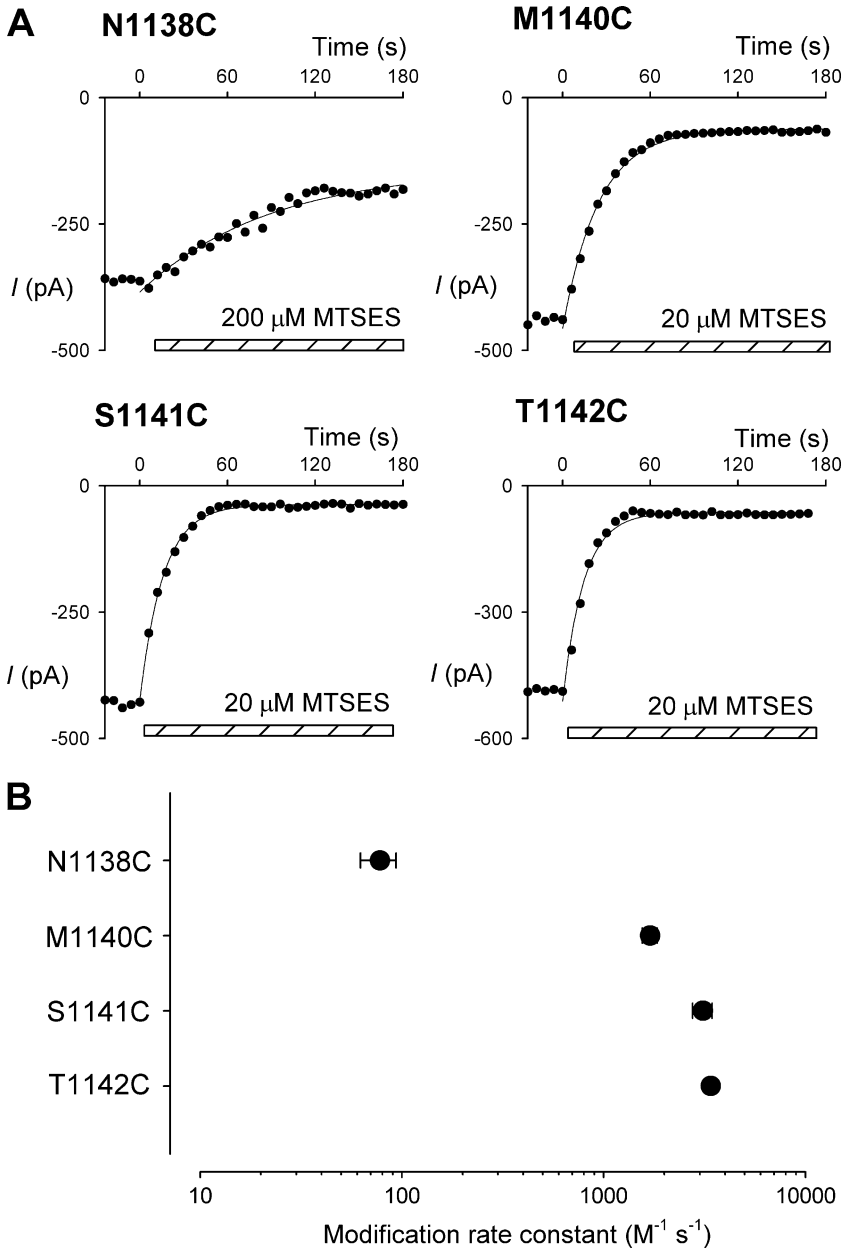

Fig. 3 Time course of modification of open channels by MTSES. **a** Example timecourses of macroscopic current amplitudes (measured at −50 mV) carried by N1138C, M1140C, S1141C, and T1142C as indicated in inside–out membrane patches. Currents amplitudes were measured every 6 s following maximal stimulation with PKA, ATP, and PPi. In each case, MTSES at the concentration indicated was applied to the cytoplasmic face of the patch at time zero (as indicated by the *hatched bar at the bottom of each panel*). The decline in current amplitude following MTSES application has been fitted by a single exponential function in each case. **b** Calculated MTSES modification rate constant for each of these four mutants. Mean of data from three to five patches

contrast, these TMs showed apparently different patterns of modification by internally applied MTS reagents.

The rate of modification by cytoplasmically applied MTSES decreases with apparent distance into the pore (Fig. 3b), suggesting that even in open channels, some factors restrict the movement of MTSES deep into the pore. In this respect, the slow rate of modification observed in N1138C (Fig. 3b) is similar to that we reported for P99C and L102C in TM1 [41] and T338C and S341C in TM6 [9], and the much higher modification rate constant for T1142C, S1141C, and (to a lesser extent) M1140C is closer to that reported for K95C in TM1 [41] and I344C, V345C, and M348C in TM6 [9]. These "groups" of side chains with similar rates of modification may experience common factors limiting MTSES access from the cytoplasm, perhaps suggesting they are located in similar regions of the open channel pore.

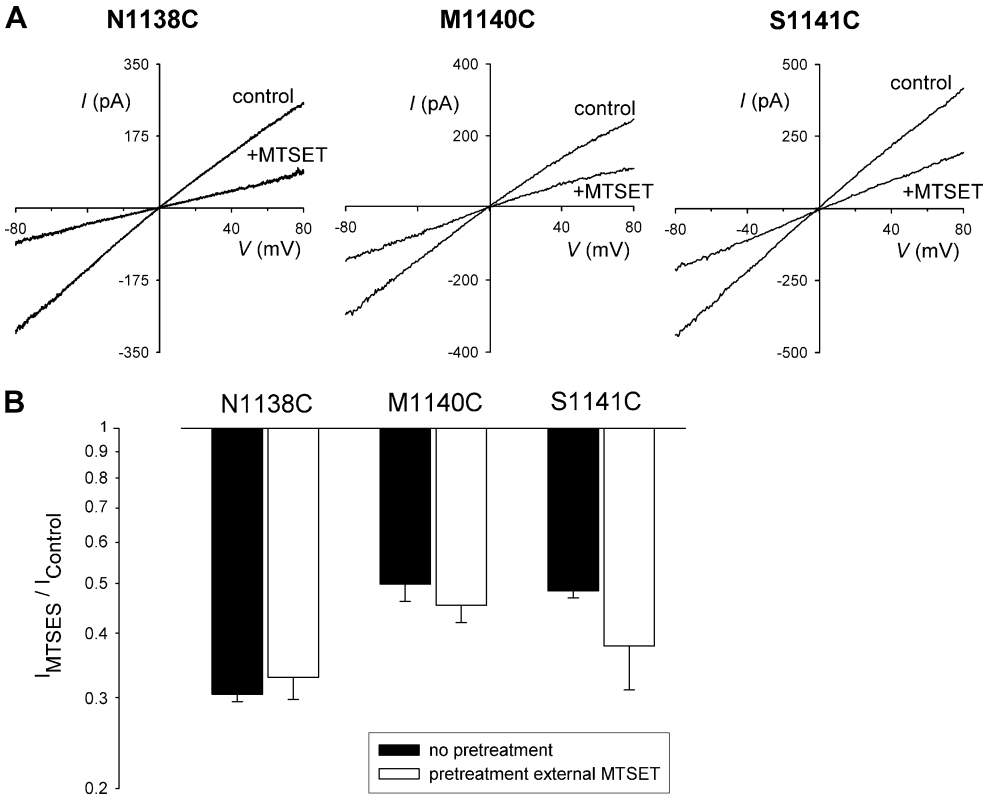

Fig. 4 No modification of introduced cysteines by external MTSET. **a** Example leak-subtracted *I–V* relationships for the three MTSET-sensitive mutants named, showing the effects of application of internal MTSET (2 mM) following maximal channel activation with PKA, ATP, and PPi. Patches were excised from cells that had been pretreated with external MTSET (5 mM, for 5 min), and showed similar sensitivity to internal MTSET as patches excised from untreated cells (for example, Fig. 1b). **b** Comparison of the effects of MTSET on macroscopic current amplitude at −80 mV between patches from untreated cells (*black bars*) and patches from cells pretreated with external MTSET (*white bars*). There were no statistically significant differences for any mutant studied ($p>0.2$). Mean of data from three to five patches

Previously, we suggested that a "barrier" within the pore prevents access of cytoplasmic substances in non-activated channels [9, 41] (Fig. 6). Using a similar approach, we find that in TM12, S1141C and T1142C can be readily modified by cytoplasmic MTSES prior to channel activation (Fig. 5), whereas N1138C and M1140C are modified rapidly after channel activation (Fig. 3) but very slowly, if at all, prior to channel activation (Fig. 5). We would therefore suggest that S1141 and T1142, like K95 in TM1 and V345 and M348 in TM6, are situated on the cytoplasmic side of the barrier and exposed to the cytoplasm in both activated and non-activated channels; whereas N1138 and M1140, like Q98, P99, and L102 in TM1 and T338, S341, and I344 in TM6, are located on the extracellular side of the barrier and exposed to the cytoplasm only following channel activation.

The proposed alignment of TM 12 with TMs 1 and 6 (Fig. 6), based on these functional data, is also consistent with previous cysteine cross-linking experiments involving TM12. Thus, a disulfide bridge can be formed between K95C in TM1 and S1141C in TM12, suggesting that the β carbon distance is in the range of ~5–8 Å for these two introduced cysteines [45]. Longer thiol-reactive cross-linking molecules have previously been shown to cross-link cysteines substituted for M348 (TM6) and T1142 (TM12), T351 (TM6), and T1142 (TM12), and W356 (TM6) and W1145 (TM12) [6].

The identification of pore-lining parts of TM12 accessible to either side of the membrane and presumably contributing to inner and outer vestibules of the pore, as well as the approximate orientation of this TM relative to other pore-lining TMs 1 and 6, extends our developing model of functional pore architecture based on functional investigation of cys-less CFTR (Fig. 6). While TMs 1, 6, and 12 all line the CFTR channel pore, the putative alignment illustrated in Fig. 6 suggests that there are important differences in their contributions to the pore. For example, whereas both TM6 and TM12 contribute many amino acid side chains to the lining of the inner vestibule of the pore on the cytoplasmic side of the putative activation "barrier," the contribution of TM1 is

Fig. 5 State-dependent modification of introduced cysteines during pretreatment with internal MTSES. **a**–**c** Example leak-subtracted *I–V* relationships for each of the four MTSES-sensitive mutants named, showing the effects of application of internal MTSES (200 μM) following maximal channel activation with PKA, ATP, and PPi. Patches have been pretreated in three different ways (see "Materials and methods"): **a** no pretreatment, **b** pretreated with MTSES (200 μM), PKA, and ATP for 2 min, and **c** pretreated with MTSES alone (200 μM) for 2 min. Note that for each mutant, following pretreatment with MTSES, PKA, and ATP, stimulated currents appeared refractory to the effects of internally applied MTSES (**b**), suggesting that channels had been covalently modified during the pretreatment. **d** Mean effect of internal MTSES on macroscopic current amplitude at +80 mV under three different sets of condition as indicated: no pretreatment (**a**), pretreated with MTSES, PKA, and ATP (**b**), and pretreated with MTSES alone (**c**). *Asterisks* indicate a significant difference from control (no pretreatment) conditions ($p<0.005$); other groups not marked by an asterisk showed no significant difference from control conditions ($p>0.1$). Mean of data from three to five patches

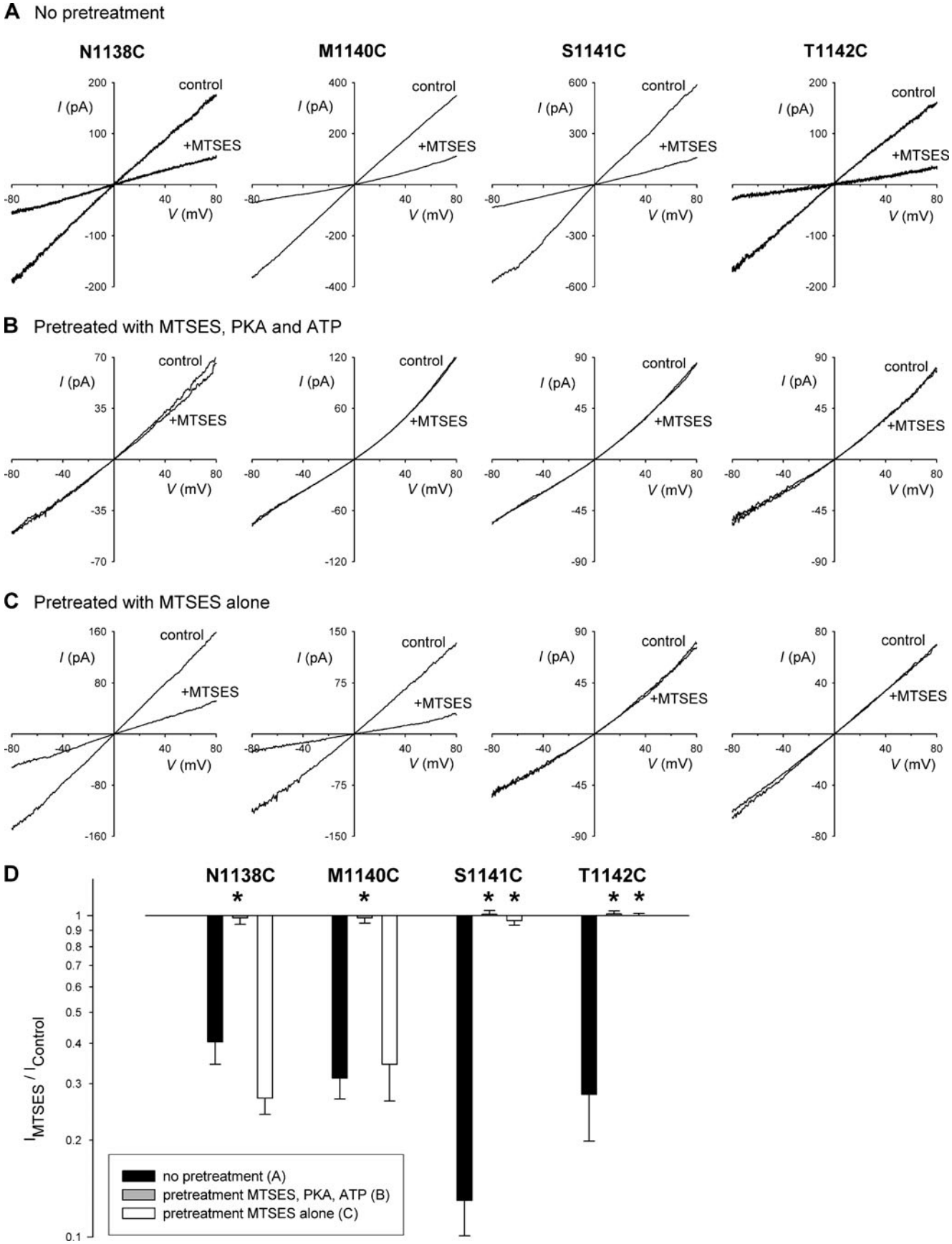
A No pretreatment
N1138C
M1140C
S1141C
T1142C
control
+MTSES
I (pA)
V (mV)
B Pretreated with MTSES, PKA and ATP
C Pretreated with MTSES alone
D
I MTSES / I Control
no pretreatment (A)
pretreatment MTSES, PKA, ATP (B)
pretreatment MTSES alone (C)

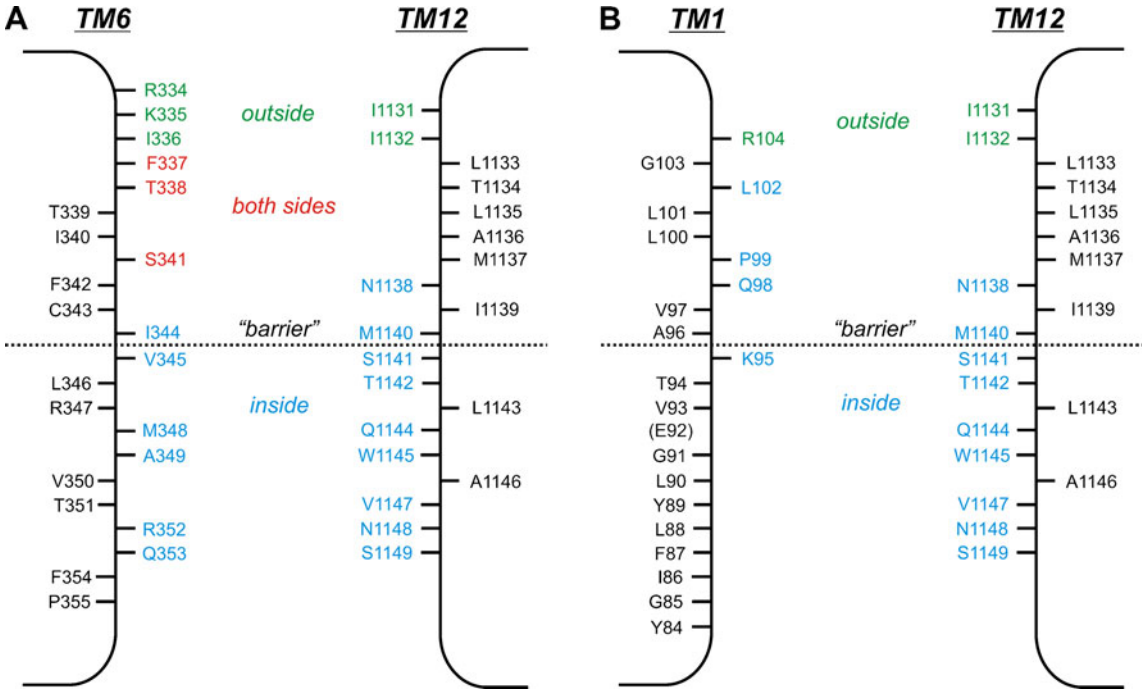

Fig. 6 Proposed locations of pore-lining side chains in TM1, TM6, and TM12 of cys-less CFTR. The proposed location of TM12 residues that are exposed to cytoplasmic MTS reagents, as described in Fig. 2, are indicated in *blue*. Note that these residues were apparently not modified by extracellular MTSET (Fig. 4). Residues that were previously shown to be modified by extracellular MTS reagents [11] are shown in *green*. Other residues that we find not to be modified by intracellular or extracellular MTS reagents and are presumed to be non-pore lining, are shown in *black*. The pattern of MTS sensitivity is compared to previously published work in TM6 (**a**) (see [9]) and in TM1 (**b**) (see [41]). Note that in TM6, some residues were found to be sensitive to both intracellular and extracellular MTS reagents; these sites are colored *red*. The putative location of a "barrier" to access in non-activated channels is also indicated; prior to channel activation, cytoplasmically applied MTSES is apparently restricted to residues below (on the intracellular side of) the barrier, whereas after channel activation, intracellular MTSES can access all side chains colored *blue* or *red*

exclusively close to and on the extracellular side of this barrier (Fig. 6). Furthermore, the pattern of side chain accessibility in the putative narrow region of the pore is very different for these three TMs. As described above, five inaccessible TM12 residues (L1133–M1137) are interposed between the externally accessible I1132 and the internally accessible N1138, possibly forming a relatively constricted region of the pore that is too narrow to accommodate bulky MTS reagents. This represents a much larger gap between externally and internally accessible side chains than was reported for TMD-1 regions TM1 and TM6 [9, 41]. In TM1, there is a very sharp divide between external (R104) and internal (L102) residues (Fig. 6b). In TM6, the boundary between outside and inside parts of the pore is even less distinct—there are three sites (F337, T338, and S341) at which cysteine residues were found to be accessible to MTS reagents applied to either side of the membrane [9] (Fig. 6a). There is good functional evidence that this part of TM6 lines the narrowest part of the open channel pore in wild-type CFTR [22], and the barrier presented to movement of MTS reagents through this part of each of TMs 1, 6, and 12 in cys-less CFTR is also consistent with this region forming the most constricted part of the pore (see above). If TM6 residues in this supposed narrow pore region are accessible from either side of the membrane, then why are side chains in the analogous part of its TMD-2 counterpart TM12 apparently accessible from neither side of the membrane? It is possible that the TM12 region L1133–M1137 does line the narrow part of the pore but that cysteines introduced in this region are non-reactive with MTS reagents or that modification does occur but is without functional consequence. This second possibility seems the least likely, since MTS modification of side chains in the same region of TMs 1 and 6 has large effects on macroscopic current amplitudes [9, 41], and it seems unlikely that deposition of a large, charged MTS reagent within the narrow pore region would not affect Cl^- permeation. It is possible that the pore lumen in this region could be too narrow to allow bulky MTS reagents to access pore-lining cysteine side chains. Again, this would be a striking contrast to the situation in TM6, where pore-lining cysteine side chains in this part of the pore can be modified by MTS reagents from either side of the membrane. One possible explanation of this discrepancy is that TM6 might show a greater flexibility or conformational movement, allowing it to adopt positions that interact with either internal or external MTS reagents. If this were the case, we would have to assume that this range of flexibility or conformational

movement was not shared by TM12—a potentially important difference between these two analogous TMs. Understanding the reasons for the apparent difference in the contribution of TM6 and TM12 to the narrow pore region will require better understanding of why TM6 residues can be modified by MTS reagents applied to either side of the membrane, given that these reagents cannot pass through the pore.

Alternatively, the different pattern of modification of cysteines in the putative narrow region of the pore (Fig. 6) might reflect that this region is lined by side chains from TMs 1 and 6, but none from TM12. It could be speculated that the narrow region is lined by fewer pore-forming TMs than the wider inner and outer vestibules. Furthermore, it has already been suggested that the contribution of different TMs varies over the length of the pore. For example, TM1 makes an important contribution to the outer part of the pore but apparently does not line the inner vestibule cytoplasmic to K95 (Fig. 6b).

While the model of functional pore architecture based on functional investigation of cys-less CFTR (Fig. 6) has implications for the structure of the open channel pore, it is difficult to put into a direct structural context. The structure of the CFTR pore region has been observed directly only at low resolution [33, 42]. Atomic homology models have been used to give a three-dimensional image of the pore-forming TMDs [3, 34, 35, 37]; however, these models have not been subjected to extensive experimental testing and may be inconsistent with existing functional data (see below). CFTR has been modeled in the "outward facing" conformation using the crystal structure of the bacterial ABC protein Sav1866 as a template [3, 34, 37] and in the "inward facing" conformation using another bacterial ABC protein template, MsbA [35]. It was suggested that the "outward facing" conformation, in which the pore is open to the extracellular side of the membrane and constricted only at the cytoplasmic end of the TMDs, represents the open state of the channel, while the "inward facing" conformation, in which the TMs are much more parallel and closely associated, represents the closed state [35]. However, there are major discrepancies between the outward facing structure and the functional model of the open channel shown in Fig. 6. In the Sav1866-based outward-facing model, residues in the central part of TM12, including N1138 and S1141, appear exposed to the extracellular solution [35], whereas our functional work indicates that these residues are exposed to the intracellular, but not the extracellular solution in open channels (Figs. 4 and 6). Our model predicts that the narrowest part of the pore is located near the extracellular end of the TMs, likely between TM12 residues L1133 and M1137 (Fig. 6; see above), a region that is wide open to the extracellular solution in the outward facing structure. As discussed previously [4, 41], the outward facing model is also in conflict with long-standing functional evidence that the open channel pore has a deep, wide inner vestibule that is open to the cytoplasm [22]. Furthermore, our suggestion that the channel is gated by a "barrier" at the level of K95/Q98(TM1)—I344/V345(TM6)—M1140/S1141(TM12) would suggest that channel opening is associated with a physical widening of this part of the pore, cytoplasmic to the narrow pore region, rather than dilation of the outer end of the TMDs. According to our functional data, residues located on the cytoplasmic side of the "barrier" are exposed to the cytoplasm in both open and closed channels [9, 41] (Fig. 5), suggesting a wide open inner pore mouth in both open and closed channels.

Because of the strong sensitivity of wild-type CFTR to internally applied MTS reagents [39], it was necessary for us to carry out our experiments using a cys-less CFTR that contains many individual amino acid changes from wild-type CFTR (see "Materials and methods"). Nevertheless, the functional properties of cys-less and wild-type CFTR appear very similar [3, 8, 19, 32], leading us [9, 41, 45] and others [3–5] to consider cys-less a good model of the wild-type CFTR pore region. However, differences in pore properties do exist between wild-type and cys-less CFTR, with cys-less showing a significantly higher single channel conductance [8, 19, 32]. It is possible, therefore, that the movement of MTS reagents in the pores of these two channel variants might be different, potentially clouding the applicability of our findings to the wild-type CFTR pore.

Our demonstration that TM12 makes a major contribution to the lining of the inner vestibule of the cys-less CFTR pore seems in apparent contradiction to previous evidence that this TM does not make an important contribution to the functional properties of the wild-type CFTR pore (see "Introduction"). Interestingly, substitution of three of the TM12 residues we identify as pore lining (N1138, S1141, and T1142) by alanine did not affect the unitary Cl^- conductance of wild-type CFTR, and had negligible effects on other permeation properties [15]. However, charge-conservative mutations in the analgous part of TM6—for example, in I344C, V345C, M348C, and A349C—also failed to significantly alter Cl^- conductance [4]. It may be, therefore, that the properties of the inner vestibule have little influence over conductance, apart from the known Cl^- concentrating effect of positively charged amino acids in this region [21, 39, 45]. Mutagenesis of S1141 does affect interactions with open channel blockers [15, 31, 45], consistent with the side chain at this position being exposed within the inner vestibule of the pore where blockers are thought to bind [45].

Whereas charge-conservative mutations in the inner vestibule have little effect on conductance, this parameter is highly sensitive to mutations in the narrow pore region. Thus, dramatic changes in conductance of wild-type CFTR

are associated with charge-conservative mutations at Q98 [13], P99 [13, 38], F337 [20], T338 [27], and S341 [31], all of which line the narrow pore region in our model (Fig. 6). In contrast, mutations in the analogous part of TM12 have been found to have little effect on conductance, which was reported as being unaltered in T1134A and M1137A [15] and slightly decreased in the less conservative T1134F [31]. The narrow pore region is also thought to determine anion selectivity [22], with significant changes in permeability to different anions being associated with mutagenesis of pore-lining TM6 residues F337 [26], T338 [27], and S341 [30]. In contrast, only very minor changes in anion permeability are associated with mutagenesis of TM12 residues T1134, M1137, and N1138 [15, 30]. It is tempting to speculate that the lack of apparent functional effect previously associated with mutagenesis of TM12 residues results, at least in part, from failure of TM12 to contribute to the narrow pore region where important functional parameters, such as Cl^- conductance and anion selectivity, might be primarily determined. If this were the case then, in spite of their overall similar positions in the membrane-spanning portion of the CFTR protein, the functional asymmetry long associated with TM6 in TMD-1 and TM12 in TMD-2 might be supposed to reflect a subtle structural asymmetry in the narrow part of the pore.

Acknowledgments This work was supported by the Canadian Institutes of Health Research and Cystic Fibrosis Canada (CFC). Yassine El Hiani is a CFC postdoctoral fellow.

References

1. Akabas MH (1998) Channel-lining residues in the M3 membrane-spanning segment of the cystic fibrosis transmembrane conductance regulator. Biochemistry 37:12233–12240
2. Akabas MH, Kaufmann C, Cook TA, Archdeacon P (1994) Amino acid residues lining the chloride channel of the cystic fibrosis transmembrane conductance regulator. J Biol Chem 269:14865–14868
3. Alexander C, Ivetac A, Liu X, Norimatsu Y, Serrano JR, Landstrom A, Sansom M, Dawson DC (2009) Cystic fibrosis transmembrane conductance regulator: using differential reactivity toward channel-permeant and channel-impermeant thiol-reactive probes to test a molecular model for the pore. Biochemistry 48:10078–10088
4. Bai Y, Li M, Hwang T-C (2010) Dual roles of the sixth transmembrane segment of the CFTR chloride channel in gating and permeation. J Gen Physiol 136:293–309
5. Beck EJ, Yang Y, Yaemsiri S, Raghuram V (2008) Conformational changes in a pore-lining helix coupled to cystic fibrosis transmembrane conductance regulator channel gating. J Biol Chem 283:4957–4966
6. Chen EY, Bartlett MC, Loo TW, Clarke DM (2004) The ΔF508 mutation disrupts packing of the transmembrane segments of the cystic fibrosis transmembrane conductance regulator. J Biol Chem 279:39620–39627
7. Cheung M, Akabas MH (1996) Identification of cystic fibrosis transmembrane conductance regulator channel-lining residues in and flanking the M6 membrane-spanning segment. Biophys J 70:2688–2695
8. Cui L, Aleksandrov L, Hou Y-X, Gentzsch M, Chen J-H, Riordan JR, Aleksandrov AA (2006) The role of cystic fibrosis transmembrane conductance regulator phenylalanine 508 side chain in ion channel gating. J Physiol 572:347–358
9. El Hiani Y, Linsdell P (2010) Changes in accessibility of cytoplasmic substances to the pore associated with activation of the cystic fibrosis transmembrane conductance regulator chloride channel. J Biol Chem 285:32126–32140
10. Fatehi M, Linsdell P (2008) State-dependent access of anions to the cystic fibrosis transmembrane conductance regulator chloride channel pore. J Biol Chem 283:6102–6109
11. Fatehi M, Linsdell P (2009) Novel residues lining the CFTR chloride channel pore identified by functional modification of introduced cysteines. J Membr Biol 228:151–164
12. Gadsby DC, Vergani P, Csanády L (2006) The ABC protein turned chloride channel whose failure causes cystic fibrosis. Nature 440:477–483
13. Ge N, Muise CN, Gong X, Linsdell P (2004) Direct comparison of the functional roles played by different transmembrane regions in the cystic fibrosis transmembrane conductance regulator chloride channel pore. J Biol Chem 279:55283–55289
14. Gong X, Linsdell P (2003) Mutation-induced blocker permeability and multiion block of the CFTR chloride channel pore. J Gen Physiol 122:673–687
15. Gupta J, Evagelidis A, Hanrahan JW, Linsdell P (2001) Asymmetric structure of the cystic fibrosis transmembrane conductance regulator chloride channel pore suggested by mutagenesis of the twelfth transmembrane region. Biochemistry 40:6620–6627
16. Gupta J, Linsdell P (2002) Point mutations in the pore region directly or indirectly affect glibenclamide block of the CFTR chloride channel. Pflügers Arch 443:739–747
17. Kidd JF, Kogan I, Bear CE (2004) Molecular basis for the chloride channel activity of cystic fibrosis transmembrane conductance regulator and the consequences of disease-causing mutations. Curr Top Dev Biol 60:215–249
18. Kos V, Ford RC (2009) The ATP-binding cassette family: a structural perspective. Cell Mol Life Sci 66:3111–3126
19. Li M-S, Demsey AFA, Qi J, Linsdell P (2009) Cysteine-independent inhibition of the CFTR chloride channel by the cysteine-reactive reagent sodium (2-sulphonatoethyl) methanethiosulphonate (MTSES). Brit J Pharmacol 157:1065–1071
20. Linsdell P (2001) Relationship between anion binding and anion permeability revealed by mutagenesis within the cystic fibrosis transmembrane conductance regulator chloride channel pore. J Physiol 531:51–66
21. Linsdell P (2005) Location of a common inhibitor binding site in the cytoplasmic vestibule of the cystic fibrosis transmembrane conductance regulator chloride channel pore. J Biol Chem 280:8945–8950
22. Linsdell P (2006) Mechanism of chloride permeation in the cystic fibrosis transmembrane conductance regulator chloride channel. Exp Physiol 91:123–129
23. Linsdell P, Gong X (2002) Multiple inhibitory effects of $Au(CN)_2^-$ ions on cystic fibrosis transmembrane conductance regulator Cl^- channel currents. J Physiol 540:29–38
24. Linsdell P, Hanrahan JW (1996) Disulphonic stilbene block of cystic fibrosis transmembrane conductance regulator Cl^- channels expressed in a mammalian cell line and its regulation by a critical pore residue. J Physiol 496:687–693
25. Linsdell P, Hanrahan JW (1998) Adenosine triphosphate-dependent asymmetry of anion permeation in the cystic fibrosis

transmembrane conductance regulator chloride channel. J Gen Physiol 111:601–614
26. Linsdell P, Evagelidis A, Hanrahan JW (2000) Molecular determinants of anion selectivity in the cystic fibrosis transmembrane conductance regulator chloride channel pore. Biophys J 78:2973–2982
27. Linsdell P, Zheng S-X, Hanrahan JW (1998) Non-pore lining amino acid side chains influence anion selectivity of the human CFTR Cl^- channel expressed in mammalian cell lines. J Physiol 512:1–16
28. Locher KP (2009) Structure and mechanism of ATP-binding cassette transporters. Phil Trans R Soc B 364:239–245
29. McCarty NA (2000) Permeation through the CFTR chloride channel. J Exp Biol 203:1947–1962
30. McCarty NA, Zhang Z-R (2001) Identification of a region of strong discrimination in the pore of CFTR. Am J Physiol 281: L852–L867
31. McDonough S, Davidson N, Lester HA, McCarty NA (1994) Novel pore-lining residues in CFTR that govern permeation and open-channel block. Neuron 13:623–634
32. Mense M, Vergani P, White DM, Altberg G, Nairn AC, Gadsby DC (2006) In vivo phosphorylation of CFTR promotes formation of a nucleotide-binding domain heterodimer. EMBO J 25:4728–4739
33. Mio K, Ogura T, Mio M, Shimizu H, Hwang T-C, Sato C, Sohma Y (2008) Three-dimensional reconstruction of human cystic fibrosis transmembrane conductance regulator chloride channel revealed an ellipsoidal structure with orifices beneath the putative transmembrane domain. J Biol Chem 283:30300–30310
34. Mornon J-P, Lehn P, Callebaut I (2008) Atomic model of human cystic fibrosis transmembrane conductance regulator: membrane-spanning domains and coupling interfaces. Cell Mol Life Sci 65:2594–2612
35. Mornon J-P, Lehn P, Callebaut I (2009) Molecular models of the open and closed states of the whole human CFTR protein. Cell Mol Life Sci 66:3469–3486
36. Rees DC, Johnson E, Lewinson O (2009) ABC transporters: the power to change. Nature Rev Mol Cell Biol 10:218–227
37. Serohijos AWR, Hegedüs T, Aleksandrov AA, He L, Cui L, Dokholyan NV, Riordan JR (2008) Phenylalanine-508 mediates a cytoplasmic-membrane domain contact in the CFTR 3D crystal structure crucial to assembly and channel function. Proc Natl Acad Sci USA 105:3256–3261
38. Sheppard DN, Travis SM, Ishihara H, Welsh MJ (1996) Contribution of proline residues in the membrane-spanning domains of cystic fibrosis transmembrane conductance regulator to chloride channel function. J Biol Chem 271:14995–15001
39. St. Aubin CN, Linsdell P (2006) Positive charges at the intracellular mouth of the pore regulate anion conduction in the CFTR chloride channel. J Gen Physiol 128:535–545
40. Vankeerberghen A, Wei L, Teng H, Jaspers M, Cassiman J-J, Nilius B, Cuppens H (1998) Characterization of mutations located in exon 18 of the *CFTR* gene. FEBS Lett 437:1–4
41. Wang W, El Hiani Y, Linsdell P (2011) Alignment of transmembrane regions in the cystic fibrosis transmembrane conductance regulator chloride channel pore. J Gen Physiol. doi:10.1085/jgp.201110605
42. Zhang L, Aleksandrov LA, Zhao Z, Birtley JR, Riordan JR, Ford RC (2009) Architecture of the cystic fibrosis transmembrane conductance regulator protein and structural changes associated with phosphorylation and nucleotide binding. J Struct Biol 167:242–251
43. Zhang Z-R, Zeltwanger S, McCarty NA (2000) Direct comparison of NPPB and DPC as probes of CFTR expressed in *Xenopus* oocytes. J Membr Biol 175:35–52
44. Zhou J-J, Fatehi M, Linsdell P (2008) Identification of positive charges situated at the outer mouth of the CFTR chloride channel pore. Pflügers Arch 457:351–360
45. Zhou J-J, Li M-S, Qi J, Linsdell P (2010) Regulation of conductance by the number of fixed positive charges in the intracellular vestibule of the CFTR chloride channel pore. J Gen Physiol 135:229–245